Nitrogen Abundant Hexaazatriphenylene-diaminobenzidine Covalent Organic Framework as Promising Cathode Material in Lithium-ion Battery

Korak Kar[a,b†], Sabiar Rahaman[c,d†], Yuchen Liu[a], Krishna D. Bhalerao[e], Hiran Jyothilal[c,d], Benjamin Duff[f], M. Dinachandra Singh[a,e], Basker Sundararaju[g], Kumar Biradha[b]* and Ashok Keerthi[a,c]**

(Dedicated to late Dr. Kanwar Singh Nalwa, a dear friend and collaborator)

[a]Department of Chemistry, School of Natural Sciences, University of Manchester, Manchester M13 9PL, UK

[b]Department of Chemistry, Indian Institute of Technology Kharagpur, Kharagpur, West Bengal, 721302, India

[c]National Graphene Institute, University of Manchester, Manchester, M13 9PL, UK

[d]Department of Physics and Astronomy, School of Natural Sciences, University of Manchester, Manchester, M13 9PL, UK

[e]Department of Sustainable Energy Engineering, Indian Institute of Technology Kanpur, Kanpur, 208016, India

[f]Manchester Institute of Biotechnology, University of Manchester, Manchester, M13 9PL, UK

[g]Department of Chemistry, Indian Institute of Technology Kanpur, Kanpur, 208016, India

† these authors contributed equally to this work as co–first authors

*Correspondence to ashok.keerthi@manchester.ac.uk, kbiradha@chem.iitkgp.ac.in, dinachandrasingh.mayanglambam@manchester.ac.uk

Keywords: Covalent Organic Frameworks, Cathode Materials, Hexaazatriphenylene, Li-ion Batteries, Energy Density

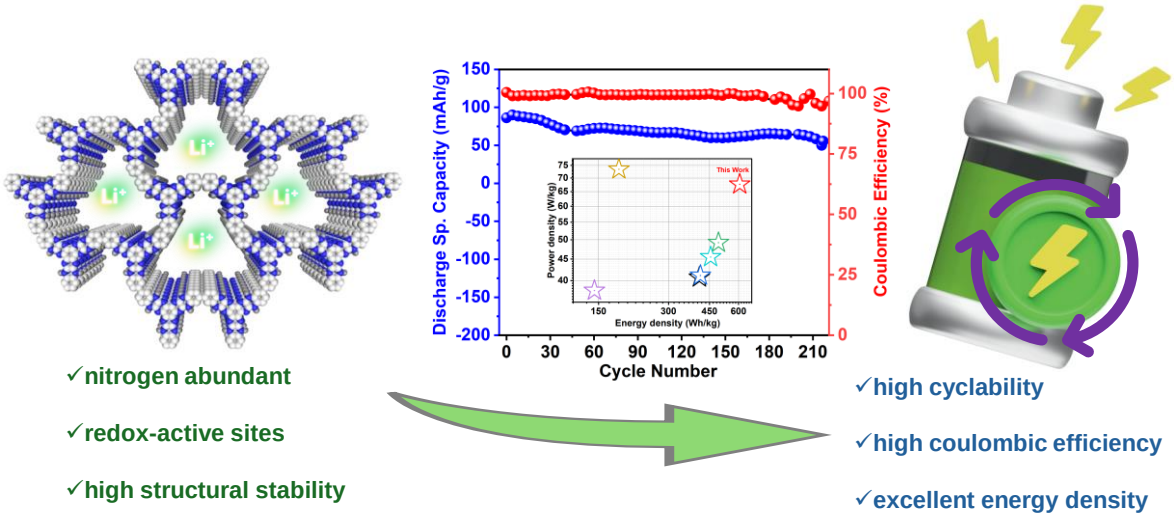

Abstract

In recent years, covalent organic frameworks (COFs) have emerged as promising materials because of their porosity, crystallinity, tunability and composition of lightweight elements. Conventionally, COFs have been mostly synthesized by reversible reactions to impart crystallinity. However, irreversible aromatic nucleophilic substitution reactions can lead to more stable materials which are much more relevant to electrochemical applications. Embedding nitrogen atoms in the rigid carbon framework in the form of phenazine and secondary arylamine moieties provides redox-active sites to the material which has been shown to provide impressive performance as cathode material in lithium-ion batteries. Herein, we report a nitrogen-rich, hexaazatriphenylene-diaminobenzidine based COF through -C-N- linkages synthesized *via* irreversible aromatic nucleophilic reactions. Due to its diverse structural features, our COF serves as a highly viable electrode material, demonstrating excellent stability and recyclability in Li-ion batteries. Our COF achieves an impressive capacity of 265 mAh/g at a current density of 0.02 A/g, with a remarkable energy density of 607 Wh/kg. Furthermore, it retains a high Coulombic efficiency of ~98% throughout the charge-discharge process even after several hundred cycles.

Introduction

In recent years, the need for high-performance rechargeable batteries has grown immensely. Reliable and sustainable energy storage systems are greatly required considering the fast-rising energy demand and the transition away from traditional fossil fuels towards renewable energy sources. Among available sources of energy storages, lithium-ion batteries (LIBs) are one of the most researched and used energy storage technologies now in use for dependable and efficient energy storage. Also, LIBs serve as the main energy source for an increasing number of electric cars and portable electronics.[1] While research in LIBs have progressed to a great extent, the basic idea for the research remains the same: decrease in the size of the battery, making the battery affordable and safe to use, and to increase the cyclic durability.[2] Typically, an anode, a cathode, a porous separating membrane and an electrolyte form the constituents of an LIB. The electrodes (cathode and anode) facilitate the movement and storage of the lithium ions through the conducting electrolyte. The porous separating membrane acts as a physical barrier to avoid contact between the cathode and anode while allowing movement of ions to prevent thermal runway. Conventionally, lithium transition metal oxides ($LiCoO_2$, $LiMnO_2$, $LiNi_xCo_yMn_{1-x-y}O_2$, etc.) have been used as cathode materials. A major limiting factor of this group of materials to be used as cathode material is their inherent low theoretical capacity, recyclability and higher cost due to the presence of metal. Commercially used anode material, graphite, has a theoretical capacity of 372 mAh/g which is relatively high compared to conventionally used cathode materials.[3] Therefore, a material that is specifically designed to achieve high theoretical capacity while maintaining excellent energy density and long-term cyclic stability is highly sought after. For LIB applications, a range of organic small molecules and polymers with redox-active functional groups have been investigated as high-performance electrode materials.[4-7] However, the fact that these polymers and organic molecules can become soluble in the electrolyte over time limits their practical usability.[8]

In 2005, Yaghi and co-workers developed the first family of COFs which are porous, crystalline, polymeric materials synthesised through specific topological design.[9] COFs are composed of lightweight elements like C, N, O, B, etc., connected by strong covalent bonds, hence, they have low density, high thermal stability and permanent porosity.[10] COFs exhibit greater stability than other crystalline materials, such as metal-organic frameworks (MOFs), in solvents and harsh conditions. This stability provides a significant advantage when used as a cathode in electrochemical cells, as it minimizes the risk of electrode material dissolution into the electrolyte over time.[10] The lightweight elements that form the backbone of COFs contribute to their higher energy density.[11-12] The intrinsic ordered structure of COFs, which imparts crystallinity, facilitates ion transport through well-defined channels, thereby enhancing the performance of cathode materials.[13]

Most synthesized COFs have been developed using reversible reactions, such as Schiff-base reactions, while COFs synthesized via irreversible reactions remain in their infancy. Reversible reactions are crucial for inducing crystallinity, as they enable continuous 'error correction' during the assembly of building blocks, ultimately leading to a thermodynamically equilibrated crystalline structure.[14] However, COFs synthesized via reversible reactions often exhibit instability, as their linkages are susceptible to hydrolysis in solvents or harsh acidic/basic conditions. In contrast, COFs formed through irreversible reactions yield significantly more robust structures.[15] The crystallinity of such COFs can be controlled by choosing the right precursors. Yaghi and co-workers had introduced irreversible aromatic nucleophilic substitution (S_NAr) reactions for COF formation.[16] Even though, the COFs are synthesised by irreversible reactions, they have crystallinity because it has annulated linkages which lead to a single possible conformation.[15] This approach of using irreversible reactions is particularly crucial in the realm of cathode material fabrication since the material must withstand harsh conditions over multiple cycles.

A particularly interesting moiety in the context of cathode material fabrication is dipyrazino-[2,3-f:20,30-h]quinoxaline or 1,4,5,8,9,12-hexaazatriphenylene (HAT). It is a planar, rigid, discotic aromatic system which has been used in diverse fields involving molecular, macromolecular and supramolecular entities.[17] HAT based materials have been used for a host of applications including catalysis[18], supercapacitors[19] and molecular sieving[20] among others. The use of HAT-based materials has been recently investigated in the domain of cathode materials for lithium-ion batteries.[21-22] HAT-based organic small molecules have been investigated as an organic cathode material in lithium-ion batteries and has shown high capacity but they fail to show good recyclability because of dissolving in the electrolyte over time.[23] Similarly, diaminobenzidine based various organic frameworks have also been explored in battery[24] and supercapacitor[25] applications.

We designed and synthesized nitrogen abundant COF through an irreversible S_NAr reaction between 1,4,5,8,9,11-Hexaazatriphenylenehexacarbonitrile (HAT-CN) and 3,3'-Diaminobenzidine (DAB) to yield HAT-DAB. The reaction gives a COF framework which is abundant in phenazine (-C=N-) and phenylimino(-NH-) moieties. These groups are essential in the process of Li^+ intercalation through the formation of various redox couples. The COF shows exceptional stability in strongly acidic and basic conditions. As a cathode material, our COF, HAT-DAB shows the highest specific capacity of 265 mAh/g at 0.02 A/g current density for the LIB applications. Interestingly, at a high current density of 1C, a capacity of ~98 mAh/g were delivered, indicating the excellent charge transfer kinetic, the presence of Li^+ ion transport channel and faster redox activities owing to COF structure. The HAT-DAB COF as a novel and pristine material demonstrates ~98% Coulombic efficiency even after 200 cycles. The slight capacity fading observed was further analyzed using non-destructive electrochemical impedance spectroscopy (EIS), revealing that electrical conductivity could be enhanced by incorporating conductive additives such as carbon nanotubes (CNTs) or reduced graphene

oxide (rGO).[26] Notably, this material achieved a remarkably high energy density of 607 Wh/kg, surpassing other reported COF materials.[27-31]

3. Results and Discussion

The COF, HAT-DAB synthesis was optimized by using re-crystalized HAT-CN and polymerisation with DAB through S_NAr type reactions under refluxing conditions in N-Methyl-2-pyrrolidone (NMP) as solvent shown in the scheme (**Figure** 1a). A ferrous sulphate ($FeSO_4$) trap was used for the liberated hydrogen cyanide (HCN) in the reaction, and it is also used to indirectly confirm the formation of the COF. The generated HCN gas reacts with $FeSO_4$ in the trap solution to form iron cyanide complex and a colour change from yellow to green (Figure S2) is observed after few hours of reaction. The IR of the green precipitate when compared to $FeSO_4$ also shows a clear C≡N stretch (Figure S4). The formation of the COF material is initially hinted by its insolubility in common solvents, as well as in strong acids and bases (Figure S3).

Comparison of the IR spectra of the precursor and the COF revealed the absence of the characteristic C≡N peak at 2242 cm^{-1} in the COF material. Additionally, the two peaks at 3385 cm^{-1} and 3354 cm^{-1}, indicative of the primary amine N-H stretch of DAB, were absent (Figure S5). Instead, a broad stretch between 3500 cm^{-1} and 3000 cm^{-1} was observed, which can be attributed to the secondary amine N-H stretch in the COF (Figure 1b).[32-33] The PXRD of the synthesized COF shows two peaks at 5.8° and 26.4°. From structural simulation (Figure S7), the former was assigned to the (100) plane and the latter to the (001) plane. The measured PXRD is closely matched with the AA stacking type in simulated stacking model (Figure S6 and S7) mainly due to missing (101) peak around 14 degrees. The broad nature of the bands is due to the short-range order of the COF.[34] Particularly, the broad peak at 26° can be assigned to the π-π stacking with a layer distance of 3.37 Å, which corresponds well with the simulated interlayer distance of 3.47 Å (Figure S6).[35] The robustness of the COF was also tested by recording the PXRD and IR after immersing it in acidic and basic media for 7 days. It was found that there is no change in the spectra indicating the high stability of the COF. This is

because of the inherent stability to the phenazine linkages in the COF which constitute of -C=N- and -C-N- bonds.[36]

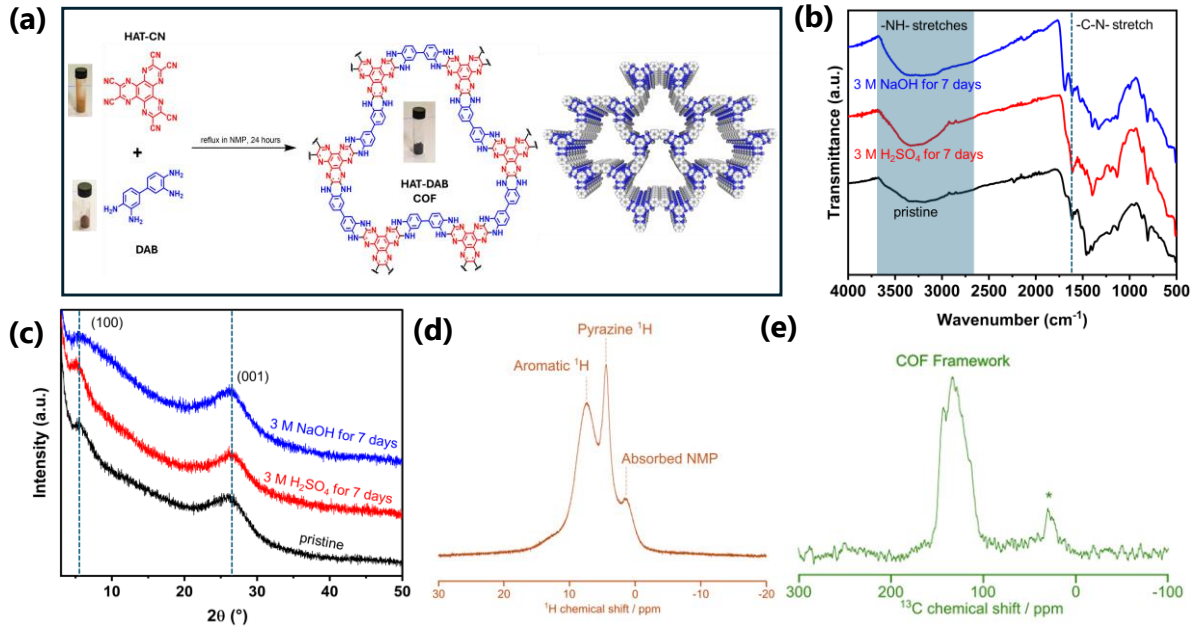

Figure 1. (a) Synthetic scheme of HAT-DAB along with schematic representation of COF chemical structure; (b) FT-IR and (c) PXRD of HAT-DAB COF, pristine (black), after acidic medium treatment (red) and after alkaline medium treatment (blue) for 7 days; (d)^{1}H Hahn-echo and (e) ^{13}C cross-polarization solid state NMR spectra collected at 16.4 T and ν_r = 60 and 20 kHz, respectively. Asterisk symbols (*) indicate spinning sidebands (see Figure S8).

Solid state NMR spectroscopy (^{13}C and ^{1}H) presented in Figure 1d and 1e were utilised to confirm the proposed structure. The ^{1}H NMR spectrum displays several resonances with the two most intense resonances at 7.4 and 4.5 ppm and integrations of 1:0.66. These resonances are consistent with the proposed structure of HAT-DAB COF (Figure 1d) and correspond to the H's associated with the aromatic moiety and the N-H in the framework.[37] The remaining resonance at around 1.5 ppm, is likely due to a small amount of residual NMP absorbed into the pores of HAT-DAB COF. The ^{13}C NMR displays a broad peak consisting of a number of

overlapping resonances across the δ range of 130-160 ppm, that can be collectively ascribed to the C=C and C=N moiety carbons of the COF framework (Figure 1e).

The nitrogen adsorption was measured for the COF at 77 K. A BET surface area of 329.6 m^2/g was obtained for the COF (Figure 2c). The surface area is in the similar range compared to related COFs reported values in literatures.[38-39] The average pore diameter description shows that most of the pores lie within the range of 1.8 - 3.2 nm (Figure 2d).

Thermogravimetric analysis (TGA) was performed to examine the thermal stability of the COF. The precursors show much pronounced weight loss and is almost completely decomposed when compared to the COF. The HAT-DAB COF undergoes a decomposition of ~53 % at 800 °C, which is impressive and higher than some other related COFs (Figure S9).[32-33] The Raman spectrum show characteristic D and G bands at 1365 cm^{-1} and 1522 cm^{-1} respectively which is in accordance with the similar kind of COFs. The D bands correspond to the sp^3 and bent sp^2 characteristics of the COF. The G band is assigned to the out of phase bending of the sp^2 carbons in the framework (Figure S10).[40]

Field emission scanning electron microscopy (FE-SEM) images show that the COF forms cluster-like aggregations (Figure 2a and 2b). The Transmission Electron Microscopy (TEM) image confirms layered structure of the HAT-DAB COF (Figure S11). High angle annular dark field- Scanning Transmission Electron Microscopy (HAADF-STEM) and corresponding electron energy loss spectroscopy (EELS) analysis (Figure S12) shows even distribution of carbon and nitrogen in the framework along with negligible amount of oxygen which is most likely due to entrapped NMP solvent molecules in the framework.

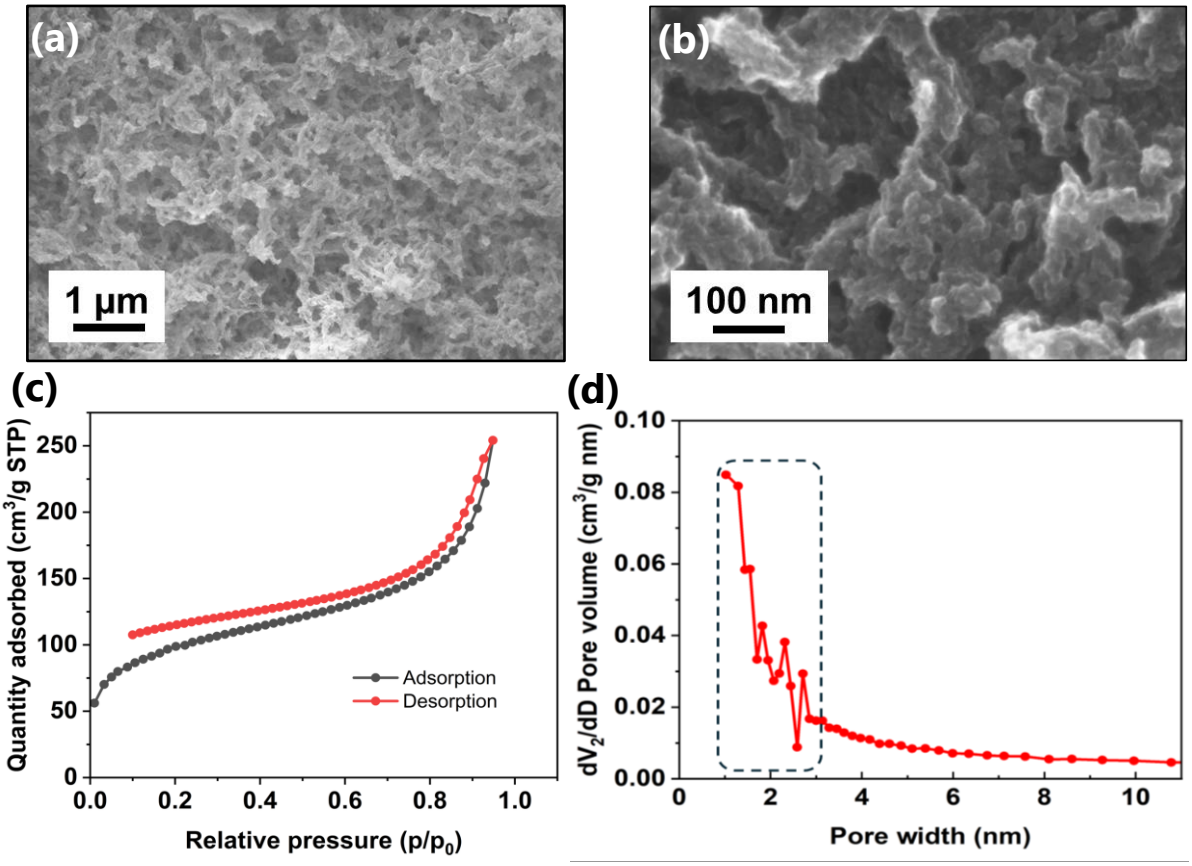

Figure 2. FE-SEM images (a,b) at various magnifications of HAT-DAB COF; (c) N_2 adsorption isotherm and (d) pore size distribution in HAT-DAB COF.

The HAT-DAB COF was tested to demonstrate their electrochemical performance as the cathode with lithium metal chip as an anode in 2032 coin cell. A cyclic voltammetry (CV) scan was initially performed over a voltage range of 1–4 V (Figure S13a) to determine the operational window of the cell. It was observed that the lower potential range predominantly contributed to charge polarization though electrical double layer capacitance (EDLC). Consequently, the electrochemical performance was investigated within an optimized voltage window of 1.5 – 4.5 V. Figure 3a shows CV scan obtained at scan rate of 0.5 mV/s over the voltage range of 1.5 - 4.5 V vs. Li/Li^+, demonstrating the formation of the SEI layer prominently. In the first cycle (light-green trace), two irreversible peaks, marked as “C” and

"D", were observed, which can be attributed to the formation of solid electrolyte interphase (SEI) layers on the cathode and similar has been reported for nitrogen rich COF material.[41]

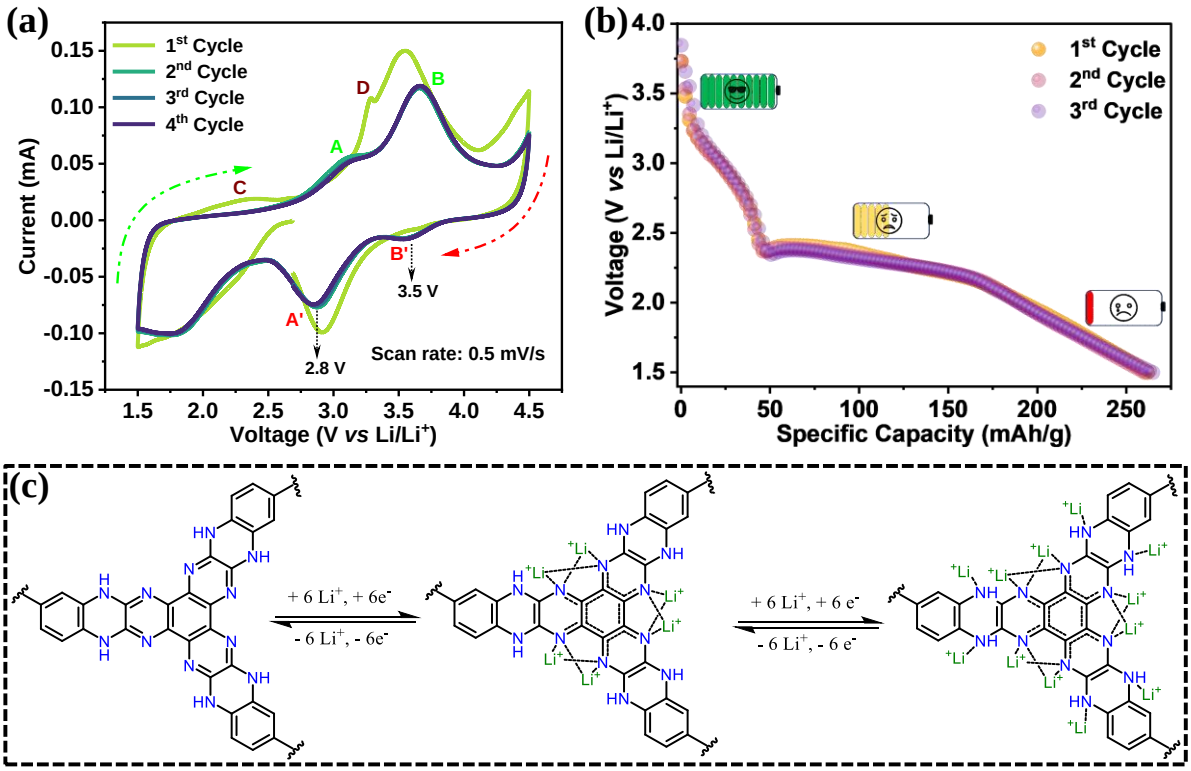

Figure 3. (a) cyclic voltammetry (CV) profiles for HAT-DAB COF-based cathode, (b) Charge−discharge profile for HAT-DAB COF cathode materials at 0.02 A/g current density, (c) plausible mechanism for lithiation/de-lithiation in the COF repeating unit.

Three consecutive CV cycles were then performed, showing two reversible redox couples. The overlapped CV cycles with two reduction peaks at 3.5 V and 2.8 V indicate lithiation at two redox sites corresponding to N-H and C=N bonds in HAT-DAB COF. Also, the charge derivative (dq/dv) plot against potential given in supplementary compliments the findings in CV scans (Figure S16). As the presence of one strong derivative peak around 2.8 V and a diminished peak at around 3.5 V suggests redox activity is more favourable around 2.8 V as compared to 3.5 V. This might be due to the decreases in total energies of COF structures as the no. of lithiation increases and thus more lithium ion is accommodated in the second discharge plateau (2.8 V), which is more than 75% of the overall capacity and a similar

mechanism has been reported.[30] Correspondingly, two distinct discharge plateaus were observed at approximately 3.36-3.12 V and 2.47-2.12 V in the galvanostatic charge/discharge plot depicted in Figure 3b. After stabilizing the SEI layers, the highest galvanostatic discharge capacity achieved was up to 265 mAh/g at a current density of 0.02 A/g. Interestingly, HAT-DAB COF exhibits a higher average discharge voltage plateau of ~2.3 V, further improving the overall energy density of the cell. In Figure 3c, plausible mechanism for Li^+ ion insertion/desertion and possible sites have been shown. Based on previously reported literature, up to 6 Li^+ ions can initially insert into the available sites, followed by an additional six Li^+ ions, totalling 12 Li^+ ion insertion sites throughout the HAT-DAB COF structure. This high capacity for Li^+ ion accommodation makes HAT-DAB COF a promising candidate for cathode materials in Li-ion batteries, offering a high theoretical capacity.[22, 42]

The rate capabilities of HAT-DAB COF were investigated at various current densities, ranging from 0.02 A/g to 0.14 A/g as shown in Figure 4a. The HAT DAB COF exhibits a high specific capacity of ~264 mAh/g at a current density of 0.02 A/g, demonstrating excellent performance under low current conditions. However, at a current density of 0.04 A/g, a sudden drop in capacity to 119 mAh/g is observed, corresponding to a 44% capacity loss. The specific capacities achieved were 119, 75, 58, 52, and 55 mAh/g at current densities of 0.04, 0.06, 0.08, 0.1, and 0.14 A/g, respectively. Notably, when the capacity was re-evaluated at a current density of 0.02 A/g, a significant decrease in capacity up to 146 mAh/g was observed compared to the initial values, with a 55 % capacity loss and suggesting structural instability at a higher discharge current rate. Thus, a minimal current of 0.04 A/g (at 0.3C) was chosen to evaluate the cycling performance for the cell as shown in Figure 4b. It is worth mentioning that HAT-DAB COF exhibited superior long-term cycling stability, as depicted in Figure 4b, maintaining a capacity of ~90.94 mAh/g with ~75% capacity retention even after 216 cycles. Further to investigate the 25% capacity loss during stability testing, we examined the voltage profile and

differential capacity (dQ/dV) *vs* voltage plot (Figure S17). In the initial cycle, three reduction peaks and one oxidation peak were observed, indicating the presence of multiple redox-active sites in the HAT-DAB COF cathode material. However, after several cycles, two reduction peaks disappeared, attended by slight peak shifting. This performance can be attributed to increased resistance at the electrode/electrolyte interphase and structural changes in the electrode (Figure S17). The deactivation of two redox-active sites resulted in only one reversible peak remaining after 216 cycles leading to reduced cyclic stability and serving as the cause of the observed capacity fade. Interestingly, the Coulombic efficiency remained approximately 98% throughout stability cycling, which signifies no loss of charge during charging/discharging.

Electrochemical impedance spectroscopy (EIS) and CV spectra were collected before and after cycling to explore the plausible mechanism of capacity fading, as shown in Figure 4c. In EIS measurements, the starting point of the semicircle at the higher frequency region corresponds to the solution resistance (R_s), and the endpoint of the semicircle is used to calculate the charge transfer resistance (R_{ct}). EIS spectra were fitted using EC Lab's Z-fit software (fitted circuit in the inset of Figure 4c), and it was observed that the solution resistance (R_s) increased from 0.28 Ω to 37.80 Ω. The R_{ct} value increased drastically from 744.9 Ω to 2000 Ω over cycling, possibly due to the decline of Li^+ ion diffusion through the SEI layer to the cathode material. EIS was also measured after the charging and discharging cycles. The charge-transfer resistance was lower when measured after discharging, likely due to the presence of Li+ ions on the electrode surface (Figure S14). The inset of Figure 4c shows the CV spectra collected before and after cycling, where the sharp reversible redox peaks diminished after cycling, likely due to the degradation of Li^+ redox sites over cycling leading to the less utilization of redox sites. This less utilization of redox site could be another possible reason for the capacity fading after cycling. Also, we performed the post-mortem analysis, and

the morphology of the cathode material surface is almost intact with some minimal crack observed after cycling shown in Figure S15, proves the mechanical strength and suitability of the material as cathode material.

In Figure 4d, we demonstrate the Ragone plot, depicting energy versus power density and comparison with other reported COFs.[27-29] The energy density was estimated of ~607 Wh/kg by considering the reversible capacity and the average discharge plateau voltage, which is much higher than traditional commercial cathode materials such as $LiMn_2O_4$, $LiCoO_2$, and $LiFePO_4$, etc. We also achieved a significantly higher power density of ~60.72 W/kg. The higher energy density of HAT-DAB COF could play a crucial role in developing sustainable cathode materials for LIBs.

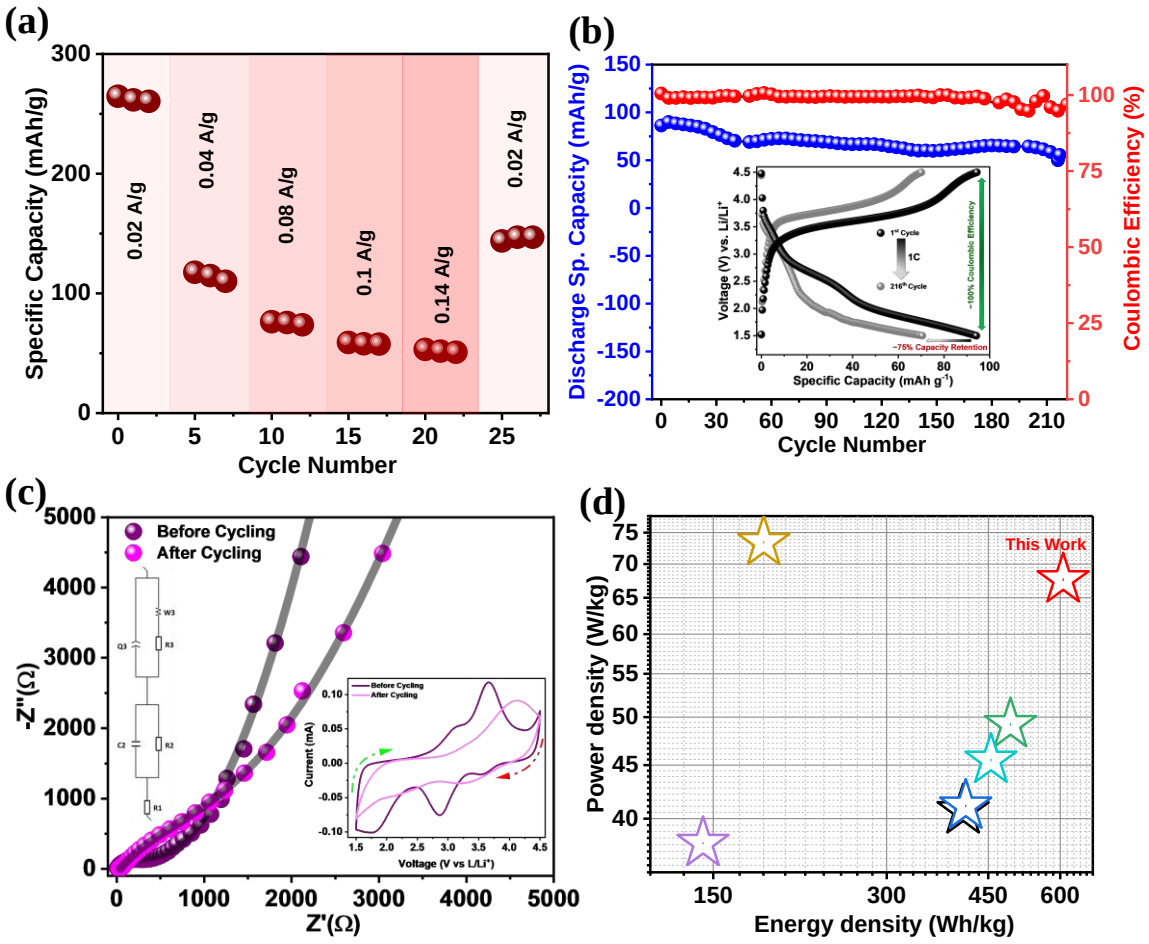

Fig. 4 (a) Rate performance, (b) Cycling stability (over 220 cycles) and the corresponding Coulombic efficiency (CE) at a rate of 1C, (inset: 1st and 216th cycles of charge-discharge

profile), (c) Nyquist plot for before and after cycling, (inset: Cyclic voltammetry plot for before and after cycling at 0.5mV/s scan rate), (d) Ragone plot to compare energy and power densities of HAT-DAB based-COF with existing literatures.[27-29]

Conclusion

We developed a new HAT-DAB covalent organic framework which shows impressive performance as a cathode material in lithium-ion batteries. The material was prepared in the solution phase with readily available chemicals through relatively fast reactions with appreciable yields which could be easily upscaled. The COF shows extremely high stability under strong acidic and basic conditions. This novel COF material possesses a comparably higher capacity of 265 mAh/g at 0.02 A/g current density. We also observed the capacity retention is ~75% even after 216 cycles with ~98% Columbic efficiency throughout the charging-discharging process. The plausible mechanism of 12 Li^+ ions accommodation, makes this COF material with higher theoretical capacity, which could be achieved with further modifications. This material demonstrated a significantly high energy density of 607 Wh/kg alongside its high capacity and stability, positioning it as a more promising candidate compared to other COF materials.

Acknowledgement

A.K. acknowledges Royal Society grant ICA\R1\231014 and Presidential Fellowship from the University of Manchester. A.K. acknowledge EPSRC strategic equipment grant EP/W006502/1. K.K. acknowledges UoM-IIT Kharagpur joint degree studentship award. This work was partly supported by the UK-India Education Research Innovation (UKIERI) award supported by British Council and SPARC India.

Conflict of interest

The authors declare no conflict of interest

Author contribution

A.K. conceived and designed the project. K.K. synthesized COF and involved in the characterisation. S.R. carried out the electrochemical experiments with help from K.D.B. Y.L. did the theoretical modelling, Raman spectroscopy and data analysis. H.J. carried out electron microscopy imaging and analysis. B.D. conducted the solid-state NMR experiments and analysis of results. A.K., K.B., M.D.S., and B.S., supervised the project and provided access to research facilities. K.K., S.R., and A.K. wrote the manuscript with inputs from all the authors.

References

1. Manthiram, A., An Outlook on Lithium Ion Battery Technology. *ACS Central Science* **2017,** *3* (10), 1063-1069.
2. Li, M.; Lu, J.; Chen, Z.; Amine, K., 30 Years of Lithium-Ion Batteries. *Advanced Materials* **2018,** *30* (33), 1800561.
3. Xu, J.; Lin, F.; Doeff, M. M.; Tong, W., A review of Ni-based layered oxides for rechargeable Li-ion batteries. *Journal of Materials Chemistry A* **2017,** *5* (3), 874-901.
4. Janoschka, T.; Hager, M. D.; Schubert, U. S., Powering up the Future: Radical Polymers for Battery Applications. *Advanced Materials* **2012,** *24* (48), 6397-6409.
5. Häupler, B.; Wild, A.; Schubert, U. S., Carbonyls: Powerful Organic Materials for Secondary Batteries. *Advanced Energy Materials* **2015,** *5* (11), 1402034.
6. Song, Z.; Zhou, H., Towards sustainable and versatile energy storage devices: an overview of organic electrode materials. *Energy & Environmental Science* **2013,** *6* (8), 2280-2301.
7. Hong, J.; Lee, M.; Lee, B.; Seo, D.-H.; Park, C. B.; Kang, K., Biologically inspired pteridine redox centres for rechargeable batteries. *Nature Communications* **2014,** *5* (1), 5335.
8. Zhu, Y.; Bai, Q.; Ouyang, S.; Jin, Y.; Zhang, W., Covalent Organic Framework-based Solid-State Electrolytes, Electrode Materials, and Separators for Lithium-ion Batteries. *ChemSusChem* **2024,** *17* (1).
9. CôTé, A. P.; Benin, A. I.; Ockwig, N. W.; O'Keeffe, M.; Matzger, A. J.; Yaghi, O. M., Porous, Crystalline, Covalent Organic Frameworks. *Science* **2005,** *310* (5751), 1166-1170.
10. Feng, X.; Ding, X.; Jiang, D., Covalent organic frameworks. *Chemical Society Reviews* **2012,** *41* (18), 6010.
11. Lohse, M. S.; Bein, T., Covalent Organic Frameworks: Structures, Synthesis, and Applications. *Advanced Functional Materials* **2018,** *28* (33), 1705553.
12. Ding, M.; Cai, X.; Jiang, H.-L., Improving MOF stability: approaches and applications. *Chemical Science* **2019,** *10* (44), 10209-10230.

13. Zhu, D.; Xu, G.; Barnes, M.; Li, Y.; Tseng, C. P.; Zhang, Z.; Zhang, J. J.; Zhu, Y.; Khalil, S.; Rahman, M. M.; Verduzco, R.; Ajayan, P. M., Covalent Organic Frameworks for Batteries. *Advanced Functional Materials* **2021,** *31* (32), 2100505.

14. Stewart, D.; Antypov, D.; Dyer, M. S.; Pitcher, M. J.; Katsoulidis, A. P.; Chater, P. A.; Blanc, F.; Rosseinsky, M. J., Stable and ordered amide frameworks synthesised under reversible conditions which facilitate error checking. *Nature Communications* **2017,** *8* (1).

15. Haase, F.; Lotsch, B. V., Solving the COF trilemma: towards crystalline, stable and functional covalent organic frameworks. *Chemical Society Reviews* **2020,** *49* (23), 8469-8500.

16. Zhang, B.; Wei, M.; Mao, H.; Pei, X.; Alshmimri, S. A.; Reimer, J. A.; Yaghi, O. M., Crystalline Dioxin-Linked Covalent Organic Frameworks from Irreversible Reactions. *Journal of the American Chemical Society* **2018,** *140* (40), 12715-12719.

17. Segura, J. L.; Juárez, R.; Ramos, M.; Seoane, C., Hexaazatriphenylene (HAT) derivatives: from synthesis to molecular design, self-organization and device applications. *Chemical Society Reviews* **2015,** *44* (19), 6850-6885.

18. Chen, X.; Liu, D.; Yang, C.; Shi, L.; Li, F., Hexaazatrinaphthalene-Based Covalent Triazine Framework-Supported Rhodium(III) Complex: A Recyclable Heterogeneous Catalyst for the Reductive Amination of Ketones to Primary Amines. *Inorganic chemistry.* **2023,** *62* (24), 9360-9368.

19. Kandambeth, S.; Jia, J.; Wu, H.; Kale, V. S.; Parvatkar, P. T.; Czaban-Jóźwiak, J.; Zhou, S.; Xu, X.; Ameur, Z. O.; Abou-Hamad, E.; Emwas, A. H.; Shekhah, O.; Alshareef, H. N.; Eddaoudi, M., Covalent Organic Frameworks as Negative Electrodes for High-Performance Asymmetric Supercapacitors. *Advanced Energy Materials* **2020,** *10* (38), 2001673.

20. Kuehl, V. A.; Yin, J.; Duong, P. H. H.; Mastorovich, B.; Newell, B.; Li-Oakey, K. D.; Parkinson, B. A.; Hoberg, J. O., A Highly Ordered Nanoporous, Two-Dimensional Covalent Organic Framework with Modifiable Pores, and Its Application in Water Purification and Ion Sieving. *Journal of the American Chemical Society* **2018,** *140* (51), 18200-18207.

21. Liu, X.; Jin, Y.; Wang, H.; Yang, X.; Zhang, P.; Wang, K.; Jiang, J., In Situ Growth of Covalent Organic Framework Nanosheets on Graphene as the Cathode for Long-Life High-Capacity Lithium-Ion Batteries. *Advanced Materials* **2022,** *34* (37), 2203605.

22. Xu, S.; Wang, G.; Biswal, B. P.; Addicoat, M.; Paasch, S.; Sheng, W.; Zhuang, X.; Brunner, E.; Heine, T.; Berger, R.; Feng, X., A Nitrogen-Rich 2D sp²-Carbon-Linked Conjugated Polymer Framework as a High-Performance Cathode for Lithium-Ion Batteries. *Angewandte Chemie International Edition* **2019,** *58* (3), 849-853.

23. Matsunaga, T.; Kubota, T.; Sugimoto, T.; Satoh, M., High-performance Lithium Secondary Batteries Using Cathode Active Materials of Triquinoxalinylenes Exhibiting Six Electron Migration. *Chemistry Letters* **2011,** *40* (7), 750-752.

24. Kraevaya, O. A.; Shchurik, E. V.; Troshin, P. A., Ni-Based Coordination Polymer as a Promising Anode Material for Potassium Batteries. *physica status solidi (a)* **2020,** *217* (12), 1901050.

25. Rahaman, S.; Kanakala, M. B.; Waldiya, M.; Sadhanala, A.; Yelamaggad, C. V.; Pandey, K., Scalable novel lanthanide-ligand complex for robust flexible micro-supercapacitors. *Journal of Power Sources* **2023,** *564*, 232801.

26. Biswas, S.; Pramanik, A.; Dey, A.; Chattopadhyay, S.; Pieshkov, T. S.; Bhattacharyya, S.; Ajayan, P. M.; Maji, T. K., 2D Covalent Organic Framework Covalently Anchored with Carbon Nanotube as High-Performance Cathodes for Lithium and Sodium-Ion Batteries. *Small* **2024**.

27. Song, Z.; Xu, T.; Gordin, M. L.; Jiang, Y.-B.; Bae, I.-T.; Xiao, Q.; Zhan, H.; Liu, J.; Wang, D., Polymer–Graphene Nanocomposites as Ultrafast-Charge and -Discharge Cathodes for Rechargeable Lithium Batteries. *Nano Letters* **2012,** *12* (5), 2205-2211.

28. Tian, D.; Zhang, H.-Z.; Zhang, D.-S.; Chang, Z.; Han, J.; Gao, X.-P.; Bu, X.-H., Li-ion storage and gas adsorption properties of porous polyimides (PIs). *RSC Advances* **2014,** *4* (15), 7506.

29. Yang, X.; Hu, Y.; Dunlap, N.; Wang, X.; Huang, S.; Su, Z.; Sharma, S.; Jin, Y.; Huang, F.; Wang, X.; Lee, S. H.; Zhang, W., A Truxenone-based Covalent Organic Framework as an All-Solid-State Lithium-Ion Battery Cathode with High Capacity. *Angewandte Chemie International Edition* **2020,** *59* (46), 20385-20389.

30. Sun, Z.; Seo, J.-M.; Liu, H.; Wei, Y.; Zhang, Y.; Li, Z.; Yao, H.; Guan, S.; Baek, J.-B., Two-dimensional fused π-conjugated multi-activity covalent organic framework as high-performance cathode for lithium-ion batteries. *Nano Energy* **2024,** *129*, 110073.

31. Lin, K.; Lin, C.-Y.; Polster, J. W.; Chen, Y.; Siwy, Z. S., Charge Inversion and Calcium Gating in Mixtures of Ions in Nanopores. *Journal of the American Chemical Society* **2020,** *142* (6), 2925-2934.

32. Lin, Y.; Cui, H.; Liu, C.; Li, R.; Wang, S.; Qu, G.; Wei, Z.; Yang, Y.; Wang, Y.; Tang, Z.; Li, H.; Zhang, H.; Zhi, C.; Lv, H., A Covalent Organic Framework as a Long-life and High-Rate Anode Suitable for Both Aqueous Acidic and Alkaline Batteries. *Angewandte Chemie International Edition* **2023,** *62* (14).

33. Kuehl, V. A.; Duong, P. H. H.; Sadrieva, D.; Amin, S. A.; She, Y.; Li-Oakey, K. D.; Yarger, J. L.; Parkinson, B. A.; Hoberg, J. O., Synthesis, Postsynthetic Modifications, and Applications of the First Quinoxaline-Based Covalent Organic Framework. *ACS Applied Materials & Interfaces* **2021,** *13* (31), 37494-37499.

34. Li, L.; Zhang, G.; Deng, X.; Hao, J.; Zhao, X.; Li, H.; Han, C.; Li, B., A covalent organic framework for high-rate aqueous calcium-ion batteries. *Journal of Materials Chemistry A* **2022,** *10* (39), 20827-20836.

35. Wang, W.; Kale, V. S.; Cao, Z.; Kandambeth, S.; Zhang, W.; Ming, J.; Parvatkar, P. T.; Abou-Hamad, E.; Shekhah, O.; Cavallo, L.; Eddaoudi, M.; Alshareef, H. N., Phenanthroline Covalent Organic Framework Electrodes for High-Performance Zinc-Ion Supercapattery. *ACS Energy Letters* **2020,** *5* (7), 2256-2264.

36. Li, X.; Cai, S.; Sun, B.; Yang, C.; Zhang, J.; Liu, Y., Chemically Robust Covalent Organic Frameworks: Progress and Perspective. *Matter* **2020,** *3* (5), 1507-1540.

37. Wang, W.; Kale, V. S.; Cao, Z.; Lei, Y.; Kandambeth, S.; Zou, G.; Zhu, Y.; Abouhamad, E.; Shekhah, O.; Cavallo, L.; Eddaoudi, M.; Alshareef, H. N., Molecular Engineering of Covalent Organic Framework Cathodes for Enhanced Zinc-Ion Batteries. *Advanced Materials* **2021,** *33* (39), 2103617.

38. Kandambeth, S.; Kale, V. S.; Shekhah, O.; Alshareef, H. N.; Eddaoudi, M., 2D Covalent-Organic Framework Electrodes for Supercapacitors and Rechargeable Metal-Ion Batteries. *Advanced Energy Materials* **2022,** *12* (4), 2100177.

39. Wang, J.; Chen, C. S.; Zhang, Y., Hexaazatrinaphthylene-Based Porous Organic Polymers as Organic Cathode Materials for Lithium-Ion Batteries. *ACS sustainable chemistry & engineering.* **2018,** *6* (2), 1772-1779.

40. Shi, R.; Liu, L.; Lu, Y.; Wang, C.; Li, Y.; Li, L.; Yan, Z.; Chen, J., Nitrogen-rich covalent organic frameworks with multiple carbonyls for high-performance sodium batteries. *Nature Communications* **2020,** *11* (1).

41. Qin, X.; Tang, H.; Zhao, H.; Shao, L.; Liu, C.; Ying, L.; Huang, F., Fully conjugated covalent organic frameworks with high conductivity as superior cathode materials for Li-ion batteries. *Journal of Materials Chemistry A* **2024,** *12* (48), 33661-33668.

42. Peng, C.; Ning, G.-H.; Su, J.; Zhong, G.; Tang, W.; Tian, B.; Su, C.; Yu, D.; Zu, L.; Yang, J.; Ng, M.-F.; Hu, Y.-S.; Yang, Y.; Armand, M.; Loh, K. P., Reversible multi-electron redox chemistry of π-conjugated N-containing heteroaromatic molecule-based organic cathodes. *Nature Energy* **2017,** *2* (7), 17074.